



# The structure and luminescence properties of green $\text{Ca}_3\text{Al}_2\text{O}_6:\text{Bi}^{3+}$ phosphors

Haidong Ju<sup>a,\*</sup>, Weiping Deng<sup>a</sup>, Baoling Wang<sup>a</sup>, Jie Liu<sup>b</sup>, Xutang Tao<sup>b</sup>, Shiqing Xu<sup>c</sup>

<sup>a</sup> Department of Chemistry, Kunming University, Kunming 650214, China

<sup>b</sup> State Key Laboratory of Crystal Institute of Crystal Materials, Shandong University, Jinan 250100, China

<sup>c</sup> College of Materials Science and Engineering, China Jiliang University, Hangzhou 310018, China

## ARTICLE INFO

### Article history:

Received 28 October 2011

Received in revised form 6 December 2011

Accepted 6 December 2011

Available online 16 December 2011

### Keywords:

Phosphors

$\text{Ca}_3\text{Al}_2\text{O}_6:\text{Bi}^{3+}$

Solid state reactions

Luminescence

Crystal structure

## ABSTRACT

A  $\text{Ca}_3\text{Al}_2\text{O}_6:\text{Bi}^{3+}$  phosphor crystallized in space group  $Pa\bar{3}$  was prepared by conventional solid state reaction at 1300 °C. The scanning electron microscopy image indicates incorporated  $\text{Bi}^{3+}$  ions cannot only enhance the growth rate of  $\text{Ca}_3\text{Al}_2\text{O}_6$  crystal, but also change the growth interface of crystal. The phosphor has two prominent emission bands at 375 nm and 490 nm. When the phosphor is excited by the 285 nm light, the 490 nm emission band predominates. However, with the increase of excitation wavelength, the intensity of the 375 nm emission band enhances. The maximum intensity of the 375 nm emission band is at  $x=0.01$  in  $\text{Ca}_{3-x}\text{Al}_2\text{O}_6:x\text{Bi}^{3+}$  phosphor while that of the 490 nm emission band is at  $x=0.03$ . There is an energy transfer process from the 375 nm emission to the 490 nm emission. Above experimental results indicate  $\text{Bi}^{3+}$  ions probably enter into different independent crystallographic sites of  $\text{Ca}^{2+}$  ions in the  $\text{Ca}_3\text{Al}_2\text{O}_6$  host lattice, and result in multiple luminescence centers. The  $\text{Ca}_3\text{Al}_2\text{O}_6:\text{Bi}^{3+}$  phosphor can be a potential green phosphor for field emission display and white light-emitting diodes.

Crown Copyright © 2011 Published by Elsevier B.V. All rights reserved.

## 1. Introduction

In recent years, phosphors have been frequently used in white light-emitting diodes, field emission display and plasma display panels. However, there are some issues that need to be improved in terms of luminescence spectrum, luminous efficiency and lifetime. In order to improve luminescence properties of phosphors, it is very important to search for good host lattices for luminescence centers. Many aluminates have been widely used as host materials for phosphors, such as  $\text{Y}_3\text{Al}_5\text{O}_{12}$  and  $\text{SrAl}_2\text{O}_4$  [1,2]. Among aluminates, the  $\text{Ca}_3\text{Al}_2\text{O}_6$  crystallized in space group  $Pa\bar{3}$  is very stable in dry air, and forms solid solutions easily with various metal oxides, such as  $\text{Cr}_2\text{O}_3$  and  $\text{SrO}$ . The substitution of the cations can result in some modifications in crystal structure, reactions conditions and luminescence properties [3]. Therefore, it is interesting to investigate the correlation between doped ions and luminescence properties of  $\text{Ca}_3\text{Al}_2\text{O}_6$  phosphors.

Trivalent bismuth cations with outer  $6s^2$  electronic configuration can enter into a variety of host lattices, and exhibit interesting luminescence properties [4,5]. A lot of literatures shows absorption bands of  $\text{Bi}^{3+}$  are usually attributed to  $^1S_0-^1P_1$  and  $^1S_0-^3P_1$  transitions that are allowed due to spin-orbit coupling [5,6]. Because the energy level of  $^3P_1$  excited state is lower than that of  $^1P_1$  excited state, the emission of  $\text{Bi}^{3+}$  ion is usually a single broad band due

to  $^3P_1-^1S_0$  transition [7]. Optical properties of  $\text{Bi}^{3+}$  ions with outer  $6s^2$  electronic configuration depend strongly on environment conditions, such as covalence, coordination number, site symmetry and space. Therefore, the luminescence of  $\text{Bi}^{3+}$  ions can vary from ultraviolet, to blue and even green by choosing appropriate hosts.

In order to search for new aluminate luminescence materials,  $\text{Ca}_{3-x}\text{Al}_2\text{O}_6:x\text{Bi}^{3+}$  phosphors were prepared by conventional solid state reaction. The crystal structure, surface morphologies, absorption spectra and luminescence spectra are reported. To understand the luminescence properties of  $\text{Bi}^{3+}$  ion in  $\text{Ca}_3\text{Al}_2\text{O}_6$  host lattice, we study multiple crystallographic independence sites of  $\text{Bi}^{3+}$  ions correlated with luminescence centers. We also optimize the luminescence intensity of the phosphors by changing  $\text{Bi}^{3+}$  concentration.

## 2. Experimental

### 2.1. Synthesis

Bismuth ions activated  $\text{Ca}_3\text{Al}_2\text{O}_6$  phosphors were prepared by conventional solid state reaction method. Starting materials consist of  $\text{CaCO}_3$  (A.R.),  $\text{Al}_2\text{O}_3$  (A.R.) and  $\text{Bi}_2\text{O}_3$  (99.9%), among which bismuth concentration ranged from 0.5 to 5 mol%. According to the nominal composition of  $\text{Ca}_{3-x}\text{Al}_2\text{O}_6:x\text{Bi}$ , the starting materials were mixed homogeneously in the appropriate molar ratio, and ground in an agate mortar. Mixtures were put into alumina crucibles in a muffle furnace, and heated from room temperature to 1300 °C at the rate of 5 °C/min. After the calcination at 1300 °C for 6 h in air, samples were naturally cooled to room temperature.

### 2.2. Characterization

The phase purity of  $\text{Ca}_3\text{Al}_2\text{O}_6:\text{Bi}^{3+}$  phosphor was checked by X-ray powder diffraction (XRD) analysis with a Bruker D8 ADVANCE diffractometer with  $\text{Cu K}\alpha$

\* Corresponding author. Tel.: +86 871 5098480.

E-mail address: [hdju1977@hotmail.com](mailto:hdju1977@hotmail.com) (H. Ju).

radiation. The UV–vis diffuse reflectance spectra were measured by a Hitachi UV-2450 spectrophotometer. The excitation and emission spectra were recorded using a Hitachi F4500 with a Xe flash lamp at room temperature. The morphologies of phosphor powders were observed using a Hitachi S-800 scanning electron microscopy (SEM).

### 3. Results and discussion

#### 3.1. XRD

Fig. 1 shows the XRD pattern of  $\text{Ca}_{2.95}\text{Al}_2\text{O}_6:0.05\text{Bi}^{3+}$  phosphor agrees well with the JCPDS 38-1429, which demonstrates that the host crystallizes in space group  $Pa\bar{3}$ . The lattice constants are  $a = 15.263 \text{ \AA}$ ,  $b = 3555.7 \text{ \AA}^{3+}$  and  $Z = 24$  [8]. According to the report of Mondal and Jeffery,  $\text{Ca}^{2+}$  ions have six independent crystallographic sites in  $\text{Ca}_3\text{Al}_2\text{O}_6$  lattice [8]. Ca (1), Ca (2) and Ca (3) are six-coordinated, and occupy centers of octahedrons, which average Ca–O band distances are 2.338, 2.392 and 2.354  $\text{Å}$ , respectively. Ca (4), Ca (5), and Ca (6) are coordinated to nine, eight and seven oxygen atoms, and average Ca–O band distances are 2.694, 2.624 and 2.525  $\text{Å}$ , respectively. The ionic radius of coordinated  $\text{Ca}^{2+}$  (1.00  $\text{Å}$ ) is very close to that of coordinated  $\text{Bi}^{3+}$  (1.03  $\text{Å}$ ), therefore,  $\text{Bi}^{3+}$  ions are expected to occupy randomly  $\text{Ca}^{2+}$  sites on account of the matching of ionic radii.

#### 3.2. SEM

All samples were prepared by the same method, however, phosphors gathered easily into a mass with increasing  $\text{Bi}^{3+}$  concentration. To investigate the influence of  $\text{Bi}^{3+}$  ions on the growth process of crystal, the SEM images of  $\text{Ca}_3\text{Al}_2\text{O}_6$  and  $\text{Ca}_3\text{Al}_2\text{O}_6:0.02\text{Bi}^{3+}$  were checked, and shown in Fig. 2. The  $\text{Ca}_3\text{Al}_2\text{O}_6$  sample without  $\text{Bi}^{3+}$  ions consists of some approximate conglomerations with an average diameter of about 0.1  $\mu\text{m}$ . When a small amount of  $\text{Bi}_2\text{O}_3$  were added to raw materials, the crystals of  $\text{Ca}_{2.98}\text{Al}_2\text{O}_6:0.02\text{Bi}^{3+}$  phosphors exhibit uniform rod-like shape with an average length of about 5  $\mu\text{m}$  and an average diameter of about 1.5  $\mu\text{m}$ . With low melt point at 820  $^\circ\text{C}$ , incorporated  $\text{Bi}_2\text{O}_3$  increases an amount of transient liquid phases that accelerate the dissolution, diffusion, and precipitation process for the crystal growth. Therefore, the incorporation of  $\text{Bi}^{3+}$  ions cannot only be helpful to enhance the growth rate of  $\text{Ca}_3\text{Al}_2\text{O}_6$  crystal, but also change the growth interface of crystal.

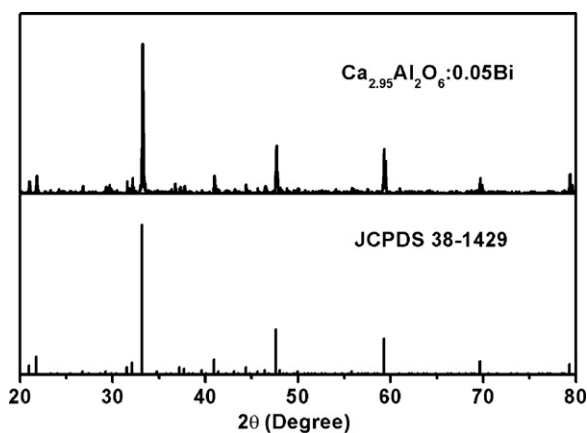


Fig. 1. The XRD pattern of  $\text{Ca}_{2.95}\text{Al}_2\text{O}_6:0.05$  phosphor as compared to the stand pattern.

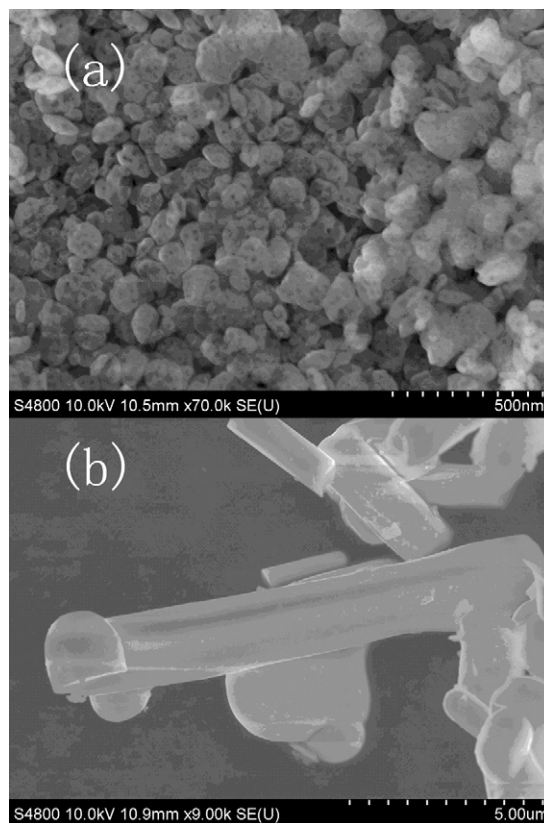


Fig. 2. The SEM images of the  $\text{Ca}_3\text{Al}_2\text{O}_6$  (a) and  $\text{Ca}_{2.98}\text{Al}_2\text{O}_6:0.02\text{Bi}^{3+}$  (b).

#### 3.3. UV–vis diffuse reflectance spectra

Fig. 3 shows diffuse reflectance spectra of  $\text{Ca}_3\text{Al}_2\text{O}_6$  host material and  $\text{Ca}_{3-x}\text{Al}_2\text{O}_6:x\text{Bi}^{3+}$  phosphors.  $\text{Ca}_3\text{Al}_2\text{O}_6$  host material without  $\text{Bi}^{3+}$  ions is white in color, and exhibits a high reflection in the visible range. The band gap energy of  $\text{Ca}_3\text{Al}_2\text{O}_6$  host is estimated to be about 3.9 eV. However, doped  $\text{Bi}^{3+}$  ions cause an immediate change in optical behavior. The spectra of  $\text{Ca}_{3-x}\text{Al}_2\text{O}_6:x\text{Bi}^{3+}$  phosphors display two absorption bands in the range of 230–400 nm. Two absorption bands are probably attributed to  $^1\text{S}_0\text{--}^3\text{P}_1$  transitions of  $\text{Bi}^{3+}$  ions in different excitation centers other than the coexistence of  $^1\text{S}_0\text{--}^3\text{P}_1$  and  $^1\text{S}_0\text{--}^1\text{P}_1$  transitions [9]. The intensities

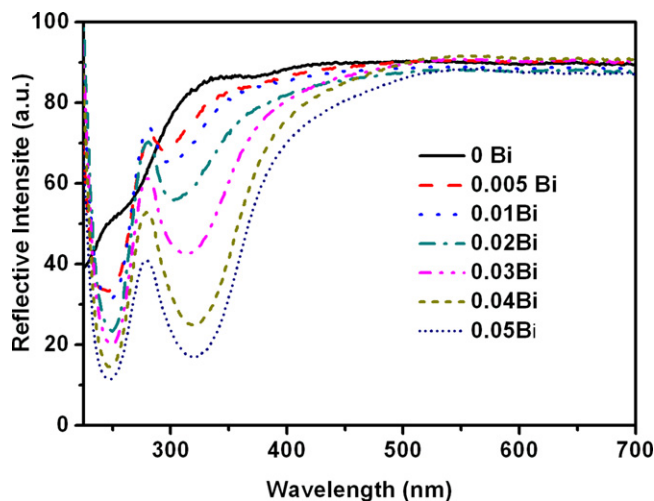


Fig. 3. The diffuse reflectance spectra for  $\text{Ca}_3\text{Al}_2\text{O}_6$  host and  $\text{Ca}_{3-x}\text{Al}_2\text{O}_6:x\text{Bi}^{3+}$  phosphors.

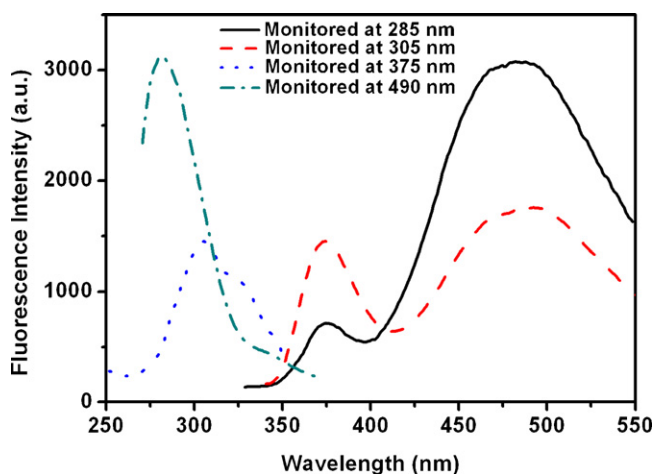


Fig. 4. The excitation and emission spectra of  $\text{Ca}_{2.99}\text{Al}_2\text{O}_6:0.01\text{Bi}^{3+}$ .

of two absorption bands increase with the enhancement of  $\text{Bi}^{3+}$  concentration. With the increase of  $\text{Bi}^{3+}$  concentration, the absorption wavelength of low energy band shows larger red-shift than that of high energy band, which indicates  $\text{Bi}^{3+}$  ions corresponding to low energy band are in a strong crystal field atmosphere.

#### 3.4. Photoluminescence

Fig. 4 displays the excitation and emission spectra of  $\text{Ca}_{2.99}\text{Al}_2\text{O}_6:0.01\text{Bi}^{3+}$  at room temperature. The phosphor has two obvious emission bands centered at 375 nm and 490 nm, among which the 490 nm emission band predominates. Two emission bands are probably attributed to the  $^1\text{S}_0-^3\text{P}_1$  transition of  $\text{Bi}^{3+}$  ions in multiple independent crystallographic sites. Monitored at 490 nm, the excitation spectrum shows a main excitation band at about 285 nm, therefore, the Stokes shift is  $15,306\text{ cm}^{-1}$ . The  $^1\text{S}_0-^3\text{P}_1$  transition of  $\text{Bi}^{3+}$  ions in weak crystal field is responsible for the excitation band at 285 nm, which is consistent with diffuse reflectance spectra. Monitored at 375 nm, the excitation spectrum consists of multiple excitation bands, among which the 305 nm excitation band predominates. The Stokes shift of 375 nm emission band is  $6120\text{ cm}^{-1}$ . The multiple excitation bands at 305 nm are ascribed to the  $^1\text{S}_0-^3\text{P}_1$  transition of  $\text{Bi}^{3+}$  ions in multiple independent crystallographic sites with strong crystal field.

To study the luminescence mechanism of  $\text{Ca}_3\text{Al}_2\text{O}_6:\text{Bi}^{3+}$  phosphor, emission spectra under different excitation lights are shown in Fig. 5. Because there are partial overlaps between 285 nm and 305 nm excitation bands, all emission spectra under different excitation lights exhibit two emission bands. With the increase of excitation wavelength, two emission peaks do not obviously shift, however, the intensity ratio of 375 nm to 490 nm emission bands always increases. There have been many reports on the  $\text{Bi}^{3+}$  activator with two emission bands in some host materials, such as  $\text{SrSb}_2\text{O}_6:\text{Bi}^{3+}$  and  $\text{YNbO}_4:\text{Bi}^{3+}$  [10,7]. Gaume-Mahn and co-workers attributed the high energy emission band (HEEB) to a charge transfer process involving  $(\text{Sb}_2\text{O}_6)^{2-}$ , and low energy emission band (LEEB) to a  $^3\text{P}_1-^1\text{S}_0$  transition of  $\text{Bi}^{3+}$  in  $\text{SrSb}_2\text{O}_6:\text{Bi}^{3+}$  [11]. Fuqiang Huang ascribed HEEB and LEEB of  $\text{SrSb}_2\text{O}_6:\text{Bi}^{3+}$  to  $^3\text{P}_1-^1\text{S}_0$  emission of isolated  $\text{Bi}^{3+}$  ions and  $\text{Bi}^{3+}$  clusters, respectively [10]. Therefore, there is no definite interpretation to HEEB and LEEB of  $\text{Bi}^{3+}$  ions, the luminescence mechanism of  $\text{Bi}^{3+}$  activators in inorganic hosts need to be further investigated. Moreover, the emission spectra of  $\text{Ca}_3\text{Al}_2\text{O}_6:\text{Bi}^{3+}$  phosphors are different from that of  $\text{SrSb}_2\text{O}_6:\text{Bi}^{3+}$  and  $\text{YNbO}_4:\text{Bi}^{3+}$  phosphors. In  $\text{SrSb}_2\text{O}_6:\text{Bi}^{3+}$  phosphors, the LEEB ( $\lambda_{\text{em}} = 487\text{ nm}$ ) results from the low energy excitation ( $\lambda_{\text{ex}} = 352\text{ nm}$ ), and the HEEB ( $\lambda_{\text{em}} = 319\text{ nm}$ )

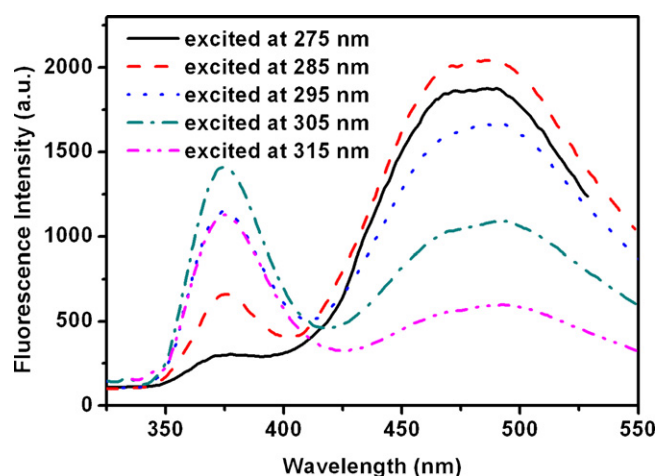


Fig. 5. The emission spectra of  $\text{Ca}_{2.95}\text{Al}_2\text{O}_6:0.005\text{Bi}^{3+}$  phosphor excited by given wavelength lights.

is caused by the high energy excitation ( $\lambda_{\text{ex}} = 301\text{ nm}$ ). However, in  $\text{Ca}_3\text{Al}_2\text{O}_6:\text{Bi}^{3+}$  phosphors, the LEEB ( $\lambda_{\text{em}} = 490\text{ nm}$ ) is assigned to the high energy excitation ( $\lambda_{\text{ex}} = 285\text{ nm}$ ), and the HEEB ( $\lambda_{\text{em}} = 375\text{ nm}$ ) results from the low energy excitation ( $\lambda_{\text{ex}} = 305\text{ nm}$ ). The difference between  $\text{Ca}_3\text{Al}_2\text{O}_6:\text{Bi}^{3+}$  phosphor and  $\text{SrSb}_2\text{O}_6:\text{Bi}^{3+}$  phosphor is probably attributed to  $\text{Bi}^{3+}$  ions in different crystallographic sites. Because Ca (1), Ca (2) and Ca (3) are all six-coordinated, and have short average Ca–O bond distances,  $\text{Bi}^{3+}$  ions substituting Ca (1), Ca (2) and Ca (3) have strong Bi–O coordinate bonds, which results in the low energy excitation band at 305 nm. Excitation states of  $\text{Bi}^{3+}$  ions chained in octahedrons have small effective space and weak relaxation effect, which are responsible for the 375 nm emission band and small Stokes shift [12]. With the same coordination number and the similar crystal field, the 375 nm emission of  $\text{Bi}^{3+}$  ions in Ca (1), Ca (2) and Ca (3) sites is composed of a single band. However, Ca (4), Ca (5) and Ca (6) have more coordinated oxygen atoms and longer average Ca–O bond distances than Ca (1), Ca (2) and Ca (3). Therefore, there are weak Bi–O coordinate bonds for substituted  $\text{Bi}^{3+}$  ions, which results in the high energy excitation band at 285 nm. With large effective space, the excited states of substituted  $\text{Bi}^{3+}$  ions shift easily to balance sites due to typical pseudo-Jahn-Teller effect [13]. The shift of  $\text{Bi}^{3+}$  excitation state results in a large Stokes shift, therefore, the emission band at 490 nm is attributed to  $^3\text{P}_1-^1\text{S}_0$  transitions of  $\text{Bi}^{3+}$  ions in Ca (4), Ca (5) and Ca (6) sites. Because Ca (4), Ca (5) and Ca (6) are even-, eight- and nine-coordinated, and have different average Ca–O bond distances, multiple emission bands make up 490 nm emission spectra.

Because the luminescence intensity of phosphor is strongly influenced by the activator concentration, the concentration of  $\text{Bi}^{3+}$  ions was experimentally studied to optimize the photoluminescence of  $\text{Ca}_{3-x}\text{Al}_2\text{O}_6:x\text{Bi}^{3+}$  phosphors. Fig. 6 shows the emission intensity as a function of  $\text{Bi}^{3+}$  concentration. The maximal intensity of the 375 nm emission band is observed in the phosphor doped with 1 mol%  $\text{Bi}^{3+}$ . A further increase of  $\text{Bi}^{3+}$  concentration results in a decrease of the emission intensity. When the  $\text{Bi}^{3+}$  concentration is in the range of 1–3 mol%, the increase of 490 nm emission intensity accompanies the decrease of the 375 nm emission intensity. Because there are partial overlaps between 285 nm excitation and 375 nm emission bands, an energy transfer from the 375 nm emission to the 490 nm emission occurs [14]. However, with increasing  $\text{Bi}^{3+}$  concentration, the intensity of the 490 nm emission band enhances until 3 mol%  $\text{Bi}^{3+}$ . The quenching of emission intensity occurs as the concentration of  $\text{Bi}^{3+}$  exceeds 3 mol%, which shows there is a nonradiative energy transfer process between  $\text{Bi}^{3+}$  ions.

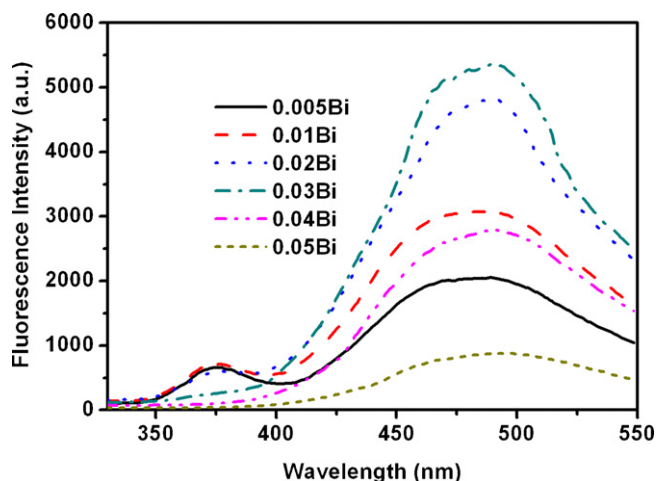


Fig. 6. The effect of the  $\text{Bi}^{3+}$  concentration on the relative luminescence intensity for  $\text{Ca}_{3-x}\text{Al}_2\text{O}_6:x\text{Bi}^{3+}$  phosphor excited by the 285 nm light.

To understand the concentration quenching, it is useful to study the critical distance ( $R_c$ ) for nonradiative energy transfer process, which can be calculated from the relation given by Blasse [15].

$$R_c \approx 2 \left[ \frac{3V}{4\pi X_c Z} \right]^{1/3} \quad (1)$$

where,  $V$  is the unit cell volume,  $X_c$  is the critical concentration, and  $Z$  is the number of formula unites per unit cell. On the basis of structural parameters,  $V = 3555.7 \text{ \AA}^3$ ,  $Z = 24$ , and  $X_c = 0.03$  for the 490 nm emission band,  $R_c$  is determined to be  $10.6 \text{ \AA}$ . The small value of  $R_c$  could be attributed to the large Stokes shift ( $15,306 \text{ cm}^{-1}$ ) resulting from the shift of  $\text{Bi}^{3+}$  excited state [16].

#### 4. Conclusions

A novel green  $\text{Ca}_3\text{Al}_2\text{O}_6:\text{Bi}^{3+}$  phosphor was prepared by conventional solid state reaction at  $1300^\circ\text{C}$  in air. When  $\text{Bi}^{3+}$  ions were doped into  $\text{Ca}_3\text{Al}_2\text{O}_6$  host lattices, crystals of sample powders grew up, and showed rod-like shape. These samples have complicated luminescence properties due to the  $\text{Ca}_3\text{Al}_2\text{O}_6$  host with six independent crystallographic sites for  $\text{Bi}^{3+}$  ions.  $\text{Bi}^{3+}$  ions with six

coordinated oxygen atoms are responsible for the 375 nm emission band and small Stokes shift ( $6120 \text{ cm}^{-1}$ ). Because of strong pseudo-Jahn-Teller effect, other  $\text{Bi}^{3+}$  ions in large spaces result in low energy emission band at 490 nm and large Stokes shift ( $15,306 \text{ cm}^{-1}$ ). There is an energy transfer process from the 375 nm emission to the 490 nm emission. When the  $\text{Bi}^{3+}$  concentration is 3 mol%, the phosphor exhibits strongest luminescence intensity at 490 nm. Therefore, the optimized  $\text{Ca}_3\text{Al}_2\text{O}_6:\text{Bi}^{3+}$  phosphor is expected to be a green candidate phosphor for field emission display and white light-emitting diodes.

#### Acknowledgements

The work was financially supported by the National Nature Science Foundation of China (51072190), the Fund of State Key Lab of Crystal Materials (KF1007), Zhejiang Province Science and Technology Program (Grant No. 2009C21020), and Yunnan Province Science and Technology Program (2010CD095).

#### Appendix A. Supplementary data

Supplementary data associated with this article can be found, in the online version, at doi:10.1016/j.jallcom.2011.12.011.

#### References

- [1] A.A. Setlur, A.M. Srivastava, *Opt. Mater.* 29 (2007) 1647–1652.
- [2] K.Y. Jung, H.W. Lee, H.K. Jung, *Chem. Mater.* 18 (2006) 2249–2255.
- [3] A.K. Prodjosantoso, B.J. Kennedy, B.A. Hunter, *Cem. Concr. Res.* 32 (2002) 647–655.
- [4] G. Blasse, A. Bril, *J. Chem. Phys.* 48 (1968) 217–222.
- [5] J. Li, J. Liu, X. Yu, *J. Alloys Compd.* 509 (2011) 9897–9900.
- [6] H. Fukada, M. Konagai, K. Ueda, T. Miyata, T. Minami, *Thin Solid Films* 517 (2009) 6054–6057.
- [7] S.H. Shin, D.Y. Jeon, K.S. Suh, *J. Appl. Phys.* 90 (2001) 5986–5990.
- [8] P. Mondal, J.W. Jeffery, *Acta Crystallogr. B* 31 (1975) 689–697.
- [9] C.H. Kim, C.H. Pyun, H. Choi, S.J. Kim, *Bull. Korean Chem. Soc.* 20 (1999) 337–340.
- [10] Y. Xia, F. Huang, W. Wang, A. Wang, J. Shi, *J. Alloys Compd.* 476 (2009) 534–538.
- [11] C. Pedrini, G. Boulon, F. Gaume-Mahn, *Phys. Stat. Sol. (a)* 15 (1973) K15–K18.
- [12] S. Zhang, Y. Nakai, T. Tsuboi, Y. Huang, H.J. Seo, *Chem. Mater.* 23 (2011) 1216–1224.
- [13] A. Bianconi, A. Valletta, A. Perali, N.L. Saini, *Physica C* 296 (1998) 269–280.
- [14] F. Clabau, X. Rocquefelte, S. Jobic, P. Deniard, M.H. Whangbo, A. Garcia, et al., *Chem. Mater.* 17 (2005) 3904–3912.
- [15] G. Blasse, *Philips Res. Rep.* 24 (1969) 131–144.
- [16] M.P. Saradhi, U.V. Varadaraju, *Chem. Mater.* 18 (2006) 5267–5272.